



## Original Articles

# A genome-wide CRISPR screen reveals that antagonism of glutamine metabolism sensitizes head and neck squamous cell carcinoma to ferroptotic cell death

Michael M. Allevato<sup>a,b,e</sup>, Sally Trinh<sup>a</sup>, Keiichi Koshizuka<sup>a</sup>, Daniela Nachmanson<sup>c</sup>, Thien-Tu C. Nguyen<sup>e</sup>, Yumi Yokoyama<sup>d</sup>, Xingyu Wu<sup>a,e</sup>, Allen Andres<sup>e</sup>, Zhiyong Wang<sup>a,e</sup>, Jeramie Watrous<sup>e</sup>, Alfredo A. Molinolo<sup>a</sup>, Prashant Mali<sup>f</sup>, Olivier Harismendy<sup>a,c</sup>, Mohit Jain<sup>e</sup>, Robert Wild<sup>d</sup>, J. Silvio Gutkind<sup>a,e,\*</sup>

<sup>a</sup> Moores Cancer Center, University of California San Diego, La Jolla, CA, USA

<sup>b</sup> Biomedical Sciences Graduate Program, University of California San Diego, La Jolla, CA, USA

<sup>c</sup> Bioinformatics and Systems Biology Graduate Program, University of California San Diego, La Jolla, CA, USA

<sup>d</sup> Dracen Pharmaceuticals Inc., 9276 Scranton Rd. Suite 200, San Diego, CA, USA

<sup>e</sup> Department of Pharmacology, University of California San Diego, La Jolla, CA, USA

<sup>f</sup> Department of Bioengineering, University of California San Diego, La Jolla, CA, USA



## ARTICLE INFO

## Keywords:

Glutamine  
Autophagy  
Ferroptosis  
Poly-unsaturated fatty acids  
Head and neck squamous cell carcinoma  
Targeted therapy  
Precision medicine

## ABSTRACT

Glutamine is a conditionally essential amino acid for the growth and survival of rapidly proliferating cancer cells. Many cancers are addicted to glutamine, and as a result, targeting glutamine metabolism has been explored clinically as a therapeutic approach. Glutamine-catalyzing enzymes are highly expressed in primary and metastatic head and neck squamous cell carcinoma (HNSCC). However, the nature of the glutamine-associated pathways in this aggressive cancer type has not been elucidated. Here, we explored the therapeutic potential of a broad glutamine antagonist, DRP-104 (sirpiglenastat), in HNSCC tumors and aimed at shedding light on glutamine-dependent pathways in this disease. We observed a potent antitumoral effect of sirpiglenastat in HPV- and HPV + HNSCC xenografts. We conducted a whole-genome CRISPR screen and metabolomics analyses to identify mechanisms of sensitivity and resistance to glutamine metabolism blockade. These approaches revealed that glutamine metabolism blockade results in the rapid buildup of polyunsaturated fatty acids (PUFAs) via autophagy nutrient-sensing pathways. Finally, our analysis demonstrated that GPX4 mediates the protection of HNSCC cells from accumulating toxic lipid peroxides; hence, glutamine blockade sensitizes HNSCC cells to ferroptosis cell death upon GPX4 inhibition. These findings demonstrate the therapeutic potential of sirpiglenastat in HNSCC and establish a novel link between glutamine metabolism and ferroptosis, which may be uniquely translated into targeted glutamine-ferroptosis combination therapies.

## 1. Statement of significance

Our study establishes a novel link between glutamine metabolism and ferroptosis and demonstrates the therapeutic potential of a broad glutamine antagonist, DRP-104 (sirpiglenastat), in head and neck cancer.

## 2. Introduction

Head and neck squamous cell carcinomas (HNSCC) arise in the oral cavity, oropharynx, and larynx and rank sixth overall in incidence, with more than 600,000 cases worldwide each year [1]. Despite advances in therapies such as immune checkpoint blockade, survival rates for patients with HNSCC have improved marginally over the past four decades, especially in oral cavity cancers associated with heavy tobacco use and alcohol consumption [2]. Multiple genetic alterations underlie

\* Corresponding author. Moores Cancer Center, University of California San Diego, 3855 Health Sciences Dr, La Jolla, CA, 92037, USA.

E-mail address: [sgutkind@health.ucsd.edu](mailto:sgutkind@health.ucsd.edu) (J.S. Gutkind).

<https://doi.org/10.1016/j.canlet.2024.217089>

Received 25 March 2024; Received in revised form 11 June 2024; Accepted 26 June 2024

Available online 2 July 2024

0304-3835/© 2024 Published by Elsevier B.V.

the development of this aggressive malignancy, including mutations and genetic alterations in the *TP53*, *FAT1*, *NOTCH1*, *CASP8*, *CDKN2A* (p16<sup>INK4A</sup>), and *PIK3CA* genes [3–6]. In particular, *PIK3CA*, which encodes the PI3K $\alpha$  catalytic subunit, is the most commonly mutated oncogene in HNSCC (~20%), aligned with our early observations that the aberrant activation of the PI3K/mTOR signaling pathway is a widespread event in HNSCC (>80% of all HPV<sup>-</sup> and HPV<sup>+</sup> cases; [7,8]). In addition, we have also observed that inhibitors of mechanistic target of rapamycin (mTOR) display potent antitumor activity in a large variety of genetically defined and chemically induced experimental HNSCC models [8–13] and our recently reported phase II clinical trial in patients with HNSCC [14]. This supports that PI3K/mTOR signaling may represent a druggable candidate in HNSCC. However, the potential immunosuppressive activity of direct mTOR inhibitors may raise safety concerns regarding their long-term use [15] or in conjunction with immunotherapies. This prompted us to focus on alternative methods of inhibition of mTOR by specifically depriving tumors of nutrients. We hypothesized that blocking key metabolic pathways would inhibit tumor growth and reveal therapeutically lethal vulnerabilities.

One of the hallmarks of cancer is its ability to alternate energetic pathways depending on its genetic profile and substrate availability [16, 17]. Cancer cells can shift from aerobic respiration (TCA cycle) to lactic acid fermentation by increasing glucose uptake and lactate production for energy production even in excess of oxygen, a phenomenon known as the Warburg Effect [18,19]. In addition, cancer cells can also shift to alternative energy sources, for example, transitioning from glycolysis or lactic acid fermentation to glutaminolysis [16,20,21]. The conversion of glutamine to lactate via glutamate, alpha-ketoglutarate, and the TCA cycle (glutaminolysis) provide many high-energy sources that complement glucose metabolism and the Warburg effect [22]. Glutaminolysis dependence may supersede glucose dependence for synthesizing specific metabolic components, leading to some cancer cells becoming addicted to glutamine catabolism [20]. This highlights the critical concept that cancer cells may exhibit metabolic vulnerabilities that can be exploited therapeutically.

Analysis of saliva and tissue metabolites from normal and HNSCC patients identified glutaminolysis pathways and its components as one of the metabolic signatures distinguishing normal from disease states [23]. Glutaminase, which catalyzes the hydrolysis of glutamine to glutamate, is also highly expressed in primary and metastatic HNSCC tissues. Glutamine is important for nucleotide synthesis, amino acid production, redox balance, glycosylation, extracellular matrix production, autophagy, and epigenetics [24,25]. Thus, glutamine metabolism may represent a critical component of HNSCC cell metabolism and a promising target to deprive of tumors. In turn, we posit that glutamine dependency may represent a potential vulnerability that could be exploited therapeutically, as single agents, or as part of synergistic strategies improving the efficacy of existing treatments.

At a serum concentration of several hundred micromolar, glutamine is one of the most abundant amino acids in the blood [24]. Rapidly proliferating cells or cells under physiological stress have a high demand for glutamine. Glutamine is transported into cells through various amino acid transporters, which tend to be upregulated in cancer [25]. Inside the cell, glutamine is metabolized by multiple processes: (i) it is hydrolyzed to glutamate and ammonia (glutaminase); (ii) it has one of its amino groups catalyzed by glutamine aminotransferases to serve as building blocks for nucleic acids, amino acids, hexosamine sugars and NAD(+); and (iii) it can charge tRNAs for protein synthesis [25]. Thus, glutamine metabolism may represent a critical component of HNSCC cell metabolism and a promising target to deprive of tumors. In turn, we posit that glutamine dependency may represent a potential vulnerability that could be exploited therapeutically, as single agents, or as part of synergistic strategies improving the efficacy of existing treatments. Targeting tumor glutamine dependence has focused on selective glutaminase inhibitors. Allosteric inhibitors such as compound 968 or CB-839 (telaglenastat) have shown promising single-agent activity in preclinical

studies [26] but had minimal single-agent anti-tumor activity in phase 2 combination trials [27]. Tumors have been shown to resist single-agent glutaminase inhibition by being extraordinarily adaptable, altering nutrient uptake and/or compensatory metabolic networks [28]. These findings favor the application of broadly active glutamine antagonists such as 6-diazo-5-oxo-L-norleucine, DON (Supplemental Fig. 1A). DON binds competitively to the active site of multiple glutamine-using-enzymes, forming a covalent adduct that irreversibly inhibits the enzyme [29]. In the clinic, DON showed promising efficacy in treating glutamine-dependent tumors, particularly with low daily doses. Still, due to non-specific exposure to the gut, stomatitis and diarrhea were consistently observed [30–33], and thus, future studies were paused. The development of DRP-104 (siripglenastat), a prodrug of DON (Supplemental Figs. 1A–B), may avoid toxicity because it is preferentially activated in the tumor microenvironment, delivering DON preferentially to the tumor while minimizing its peripheral and GI tissue exposure, leading to significantly reduced toxicity [34].

Our study explores the therapeutic implications of inhibiting glutamine metabolism in HNSCC. We investigated the effects of broad glutamine metabolism antagonism on human HNSCC cells, revealing that this blockade impairs mTOR signaling, induces autophagy, and leads to the accumulation of polyunsaturated fatty acids (PUFAs). This metabolic disturbance sensitizes cells to lipid peroxidation, triggering ferroptosis and enhancing the efficacy of ferroptosis-inducing agents. Our findings suggest that a dual approach targeting glutamine metabolism and ferroptosis could represent a potent strategy against HNSCC.

### 3. Methods

#### 3.1. Cell lines, culture procedures, and reagents

Human HNSCC cell lines CAL27, CAL33 HN12, SCC47, and Detroit 562 were obtained from the NIDCR (National Institute of Dental and Craniofacial Research) cell collection and cultured as previously reported [35]. Please see the supplemental information for the full description of the reagents used.

#### 3.2. Cell viability assay and synergy determination

Cells were seeded at a density of 5000 cells/well in 96-well plates, and 10 dilutions of each inhibitor (DON or DRP104) were assayed in technical triplicates for 72 h. Live cell number was measured with the CellTiter-Fluor Cell Viability Reagent. The half-maximal inhibitor concentration values (GI<sub>50</sub>) were determined from the curve using the nonlinear log (inhibitor) versus response-variable slope (three parameters) equation. For synergy determination, cells were treated with either single inhibitors, siRNA, or combinations thereof using six different dilutions of each inhibitor and in technical triplicates and incubated for 72 h. Live cell number was measured as above, and the Bliss independence model (BLISS-Chou) was used to determine if the interaction is additive ( $\Delta\text{Bliss} = 0$ ), synergistic ( $<0$ ), or antagonistic ( $>0$ ), respectively. Please see supplemental information for the full description.

#### 3.3. Sphere formation assay and human xenograft tumor models

Cells were seeded in 96-well ultralow attachment culture dishes and treated with the indicated concentration of 3 mM or 10 mM DON. Ten days after seeding, photos of wells were taken, and the number of spheres in each well and their sizes were assessed by bright-field microscopy and quantified using Qupath. Female 4- to 6-week-old NOD.Cg-Prkdcscid Il2rgtm1Wjl/SzJ (SCID-NOD) mice were injected subcutaneously in both flanks with  $5 \times 10^5$  of each human HNSCC cell line. Mice were monitored 3 times weekly for tumor development. After 14 days post-implantation, mice were evenly distributed by size and treated with either vehicle or DRP-104 (3 mg/kg) subcutaneously according to their weight; 5 days ON, 2 days OFF. RSL3 (100 mg/kg) was

administered intratumorally after 23 days post-implantation, twice a week for 2 weeks. The control group was treated with each vehicle. Mice were euthanized at the indicated time points, and tumors were isolated for histologic and IHC evaluation. Results of mice experiments were expressed as mean  $\pm$  SEM of a total of tumors analyzed. Please see the supplemental information for the full description.

### 3.4. Metabolite extraction and LC-MS metabolomics

CAL33 cells were prepared and analyzed by liquid chromatography with tandem mass spectrometry (LC-MS/MS) as previously described [36]. LC-MS/MS-based metabolomics analysis was performed using a Thermo QExactive orbitrap mass spectrometer coupled to a Thermo Vanquish UPLC system. For data processing, in-house R-scripts performed initial bulk feature alignment, MS1-MS2 data parsing, pseudo-DIA-to-DDA MS2 deconvolution, and CSV-to-MGF file generation. RAW to mzXML file conversion was performed using MSconvert version 3.0.9393. Feature extraction, secondary alignment, and compound identification were performed using mzMine 2.21 [37]. When available, the preliminary ID was given based on mass and retention time. Compounds identified as "EIC\_X" or "Novel\_EIC\_X" indicate compounds that were putatively identified as previously described [36]. Statistical analysis was performed using R (3.3.3). The data generated in this study are available upon request from the corresponding author.

### 3.5. Statistical analysis

All data analyses were performed using GraphPad Prism, version 9.4.0 for Mac. The data were analyzed by one-way ANOVA test with correction for multiple comparisons or *t*-test (asterisks denote: \* $p < 0.05$ , \*\* $p < 0.01$ , \*\*\* $p < 0.001$ , and \*\*\*\* $p < 0.0001$ ). All experiments were repeated independently with similar results at least three times.

Transfections, immunoblotting, immunohistochemistry, CRISPR screen and analysis and immunofluorescence.

Please see supplemental information for the full description.

### 3.6. Data availability

The code and data generated in this study are available upon request from the corresponding author.

## 4. Results

### 4.1. Glutamine metabolism blockade limits HNSCC cell line proliferation and tumorigenesis

To examine the ability of DRP-104 to inhibit HNSCC cell proliferation relative to DON, we performed a series of experiments using a panel of human cell lines representing a spectrum of human papillomavirus (HPV+) and HPV- HNSCC. Cells were treated with serial concentrations of DON or DRP-104 for 72 h in a 96-well plate (Fig. 1A). No significant changes were observed between IC<sub>50</sub> values calculated for DON and DRP104, indicating that DRP-104 was just as efficacious as DON due to these HNSCC cell lines bearing the tumor-specific enzymes required to activate the pro-drug (Fig. 1A and Supplemental Figs. 2A–B). Remarkably, HNSCC cells carrying genetic alterations in the *PIK3CA/PTEN* pathway were more sensitive to glutamine metabolism antagonism than unaltered HNSCC cells (Supplemental Figs. 2A–B).

We next investigated whether glutamine metabolism blockade could inhibit the tumorigenic potential by comparing the ability of sphere growth (orospheres) of vehicle-treated and DON-treated cells (Fig. 1B). In all HNSCC cell lines used, DON significantly reduced the number of large spheres formation; correspondingly, cell lines bearing *PIK3CA/PTEN* alterations resulted in a more pronounced reduction.

Given the ability of DON and DRP-104 to inhibit cell proliferation, we next tested the antitumor activity of DRP-104 using HNSCC

xenograft tumor models. SCID/NSG mice were injected subcutaneously with HNSCC cell lines. Orthotopic tumor implantation may have been preferable, but this can cause difficulty in eating and drinking, thus affecting overall metabolism and confounding our results. Despite this limitation, for each tumor type tested, treatment with DRP-104 led to a marked decrease in tumor growth and tumor weight and improved survival (Fig. 1C and D and Supplemental Figs. 2C–D). Due to past clinical studies reporting gastrointestinal toxicities with the drug form of DON, we measured the weight of the mice treated with the pro-drug (DRP-104) throughout our studies, finding that no changes in weight were observed (Fig. 1E and Supplemental Fig. 2E).

### 4.2. Glutamine metabolism antagonism leads to the dysregulation of autophagy and poly-unsaturated fatty acid accumulation

DON and DRP-104 can reshape the cellular metabolic and energy networks by inhibiting a wide range of glutamine-utilizing enzymes. To capture the metabolic shifts and compensations in HNSCC cells in response to glutamine metabolism, CAL33 cells were treated with DON for 24 h, and their lysates were analyzed and quantified by LC/MS/MS. As demonstrated in Supplemental Fig. 3A, the dose of DON used in these experiments did not induce cell death, ensuring that cellular mortality events did not confound our metabolic analysis. Three hundred sixty-one metabolites were identified, of which 42 (12 %) were significantly modulated by glutamine metabolism blockade, with 32 metabolites being upregulated while 10 metabolites were downregulated with treatment (Fig. 2A and Supplemental Table 1). Enrichment analysis of significant metabolites found a remarkable accumulation of metabolites derived from alpha-linolenic acid and linoleic acid, while broad nucleic-acid metabolism was depleted (Fig. 2B). To better understand the effect of glutamine metabolism antagonism on fatty acid metabolism, we examined the distribution and abundance of fatty acids in CAL33 cells following a 24-h DON treatment. In contrast to vehicle-treated cells, glutamine metabolism blockade induced a robust increase in lipid droplets, exhibiting approximately 10-fold more lipid droplets than vehicle-treated cells (Fig. 2C). To provide a comparative perspective, it is noteworthy that CAL27 cells, despite also being subjected to glutamine metabolism blockade, exhibited fewer lipid droplets than CAL33 cells, albeit still showing a significant increase (Supplemental Fig. 3A). An increase in lipid droplets during starvation has also been observed in human cells [38], suggesting

that glutamine metabolism antagonism induces a similar general cellular response to nutrient deprivation. mTOR is a central nutrient-sensitive kinase and a regulator of cell growth and autophagy [39,40]. Under sufficient amino acids, mTOR phosphorylates and prevents the activation of ULK1, a central component of the autophagy pathway (Fig. 2D) [40,41]. Conversely, mTOR is inhibited without amino acids, and autophagy is activated. Starvation-induced autophagic degradation of membranous organelles releases fatty acids, which accumulate to form lipid droplets [38] (Fig. 2D). In agreement with the inhibition of mTORC1 activity during starvation, treating CAL27 and CAL33 cells with the glutamine metabolism antagonist DON resulted in a substantial loss of phosphorylated S6, a downstream target of mTOR and hence reflecting a decrease in mTOR activity (Fig. 2E).

Additionally, we monitored the phosphorylation of ATG13 on Ser-355, which can be used as a read-out for ULK1 kinase activity in cells [39]. HNSCC cells treated with DON had higher levels of ATG13 pSer-355, indicating that ULK1 was activated, likely initiating autophagy (Fig. 2E). Moreover, the levels of p62/A170/SQSTM1 (p62), another marker of autophagy that is known to be degraded by autophagy, decreased in CAL27 and CAL33 cells treated with DON (Supplemental Fig. 3B). To further investigate the role of autophagy, we examined the expression levels LC3B in CAL27 and CAL33 cells treated with DON and the autophagy inhibitor hydroxychloroquine (HCQ). We found that DON led to increased LC3B concomitant with decreased p62 levels, aligned with enhanced autophagy (Supplemental Fig. 3B).

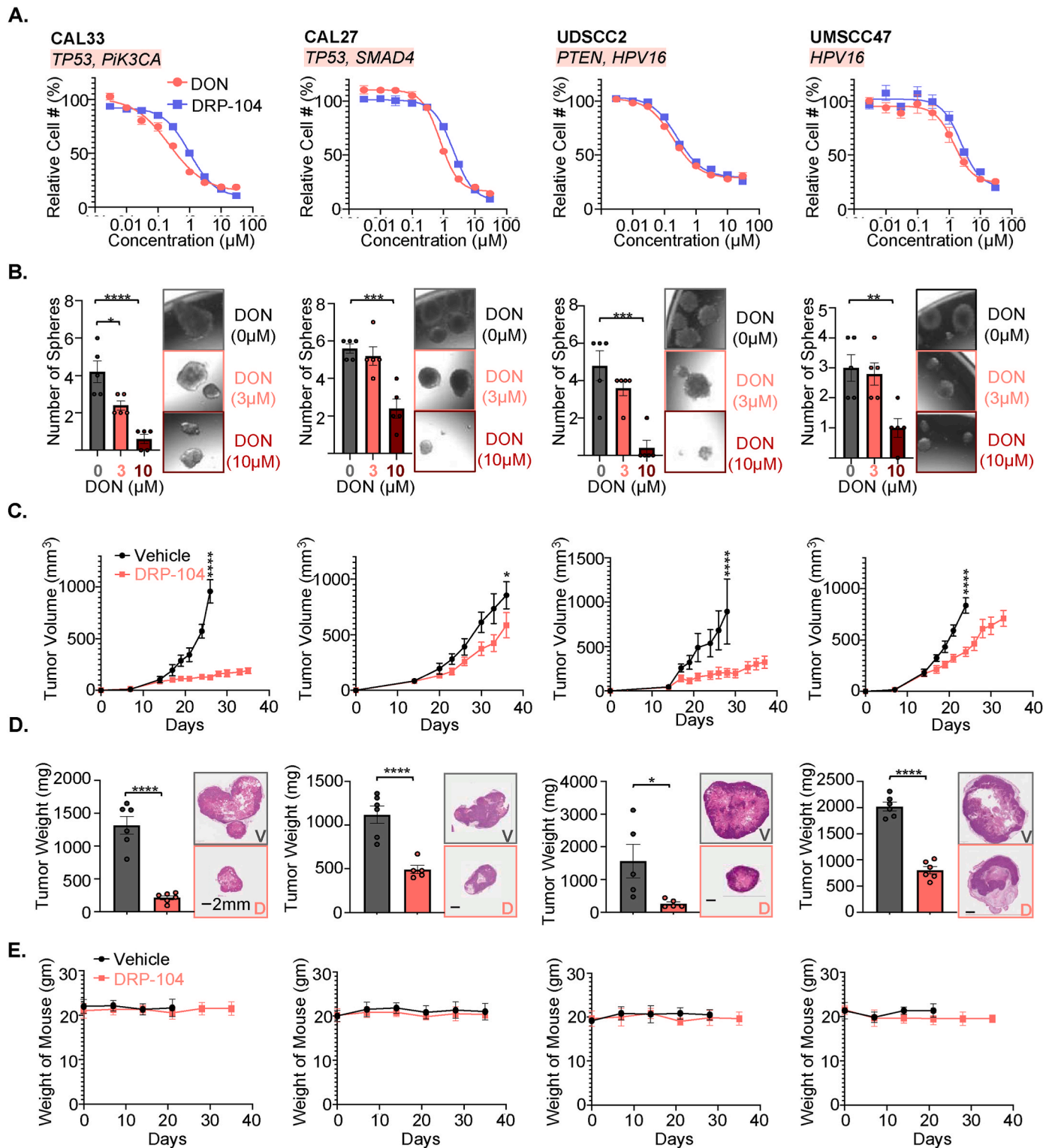


**Fig. 1.** Effects of glutamine metabolism antagonism on HNSCC tumorigenesis. A. Representative HNSCC cells (CAL33, CAL27, UDSCC2, and UMSCC47) were treated with the indicated concentrations of DON or DRP104 for 72 h. Live cell number was normalized with the corresponding vehicle control (0.1 % DMSO)-treated cells. Driver gene alterations are highlighted in red. B. HNSCC cells were treated with vehicle control (0.1 % DMSO) or DON (3 and 10  $\mu$ M). Wells were imaged, and the size/number of spheres was quantified via QuPath. Representative spheres obtained are displayed on the right. C. Corresponding cell lines were transplanted into NSG mice and treated subcutaneously with vehicle control diluent or DRP-104 (3 mg/kg) once daily 5 days-ON + 2days OFF x indicated cycles. Treatment was continued for four weeks. D. Lesions from corresponding xenograft studies were collected and weighed on day 35 ( $n = 6$  mice per group). Representative H&E images of the tumors are displayed on the right. E. Mice weight throughout each preclinical study. All data represent averages  $\pm$ SEM, except where indicated. \* $P < 0.05$ , \*\*\* $P < 0.001$ , \*\*\*\* $P < 0.0001$ .

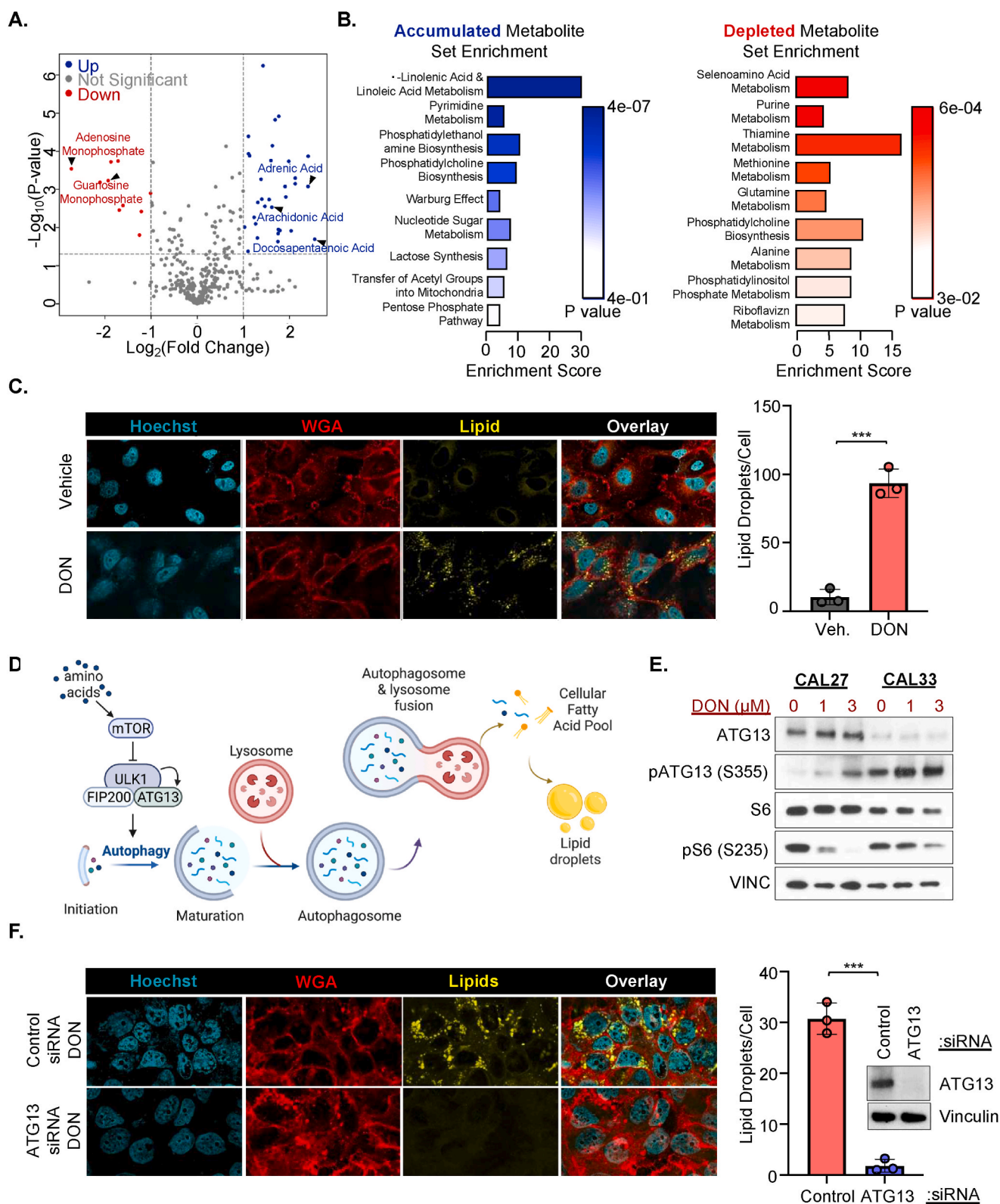


**Fig. 2. Glutamine metabolism blockade induces autophagocytotic accumulation of polyunsaturated fatty acids.** **A.** CAL33 HNSCC cells were treated with 3  $\mu$ M DON for 24 h and analyzed by HILIC LC-MS. Volcano plot depicting polar molecule, eicosanoids, and other bioactive lipid species alterations in CAL33 cells;  $n = 4$  samples per treatment group. **B.** Metabolite set enrichment analysis depicted sets of metabolites accumulated or depleted after glutamine metabolism blockade treatment with DON. **C.** CAL33 cells were treated for 24 h with DON (3  $\mu$ M). Cells were fixed and stained with Hoechst (Blue), Wheat Germ Albumin (Red), and LipidTOX™ (Yellow). Intracellular accumulation of neutral lipid droplets was quantified per cell in 4 regions of interest per replicate ( $n = 3$ ). **D.** A model illustrates that in the presence of sufficient amino acids, active mTOR inhibits the initiation of autophagy and the degradation of membranous organelles that release fatty acids. **E.** Lysates of CAL27 and CAL33 cells treated with DON (1 and 3  $\mu$ M) were analyzed for indicated proteins by western blotting. **F.** CAL33 HNSCC cells were treated with non-targeting or ATG13-siRNA and subsequently treated with DON (3  $\mu$ M) for 24 h. Neutral lipid droplets were quantified. Cell lysates of siRNA-treated cells were analyzed for indicated proteins via Western blot analysis. All data represent averages  $\pm$ SD, except where indicated. \*\*\* $P < 0.001$ .

Inhibition of autophagosome degradation by HCQ further accumulated LC3B levels. This supports the involvement of autophagy in the response to glutamine metabolism blockade. In turn, since ATG13 is essential for the stability of the ULK1-ATG13-FIP200 complex-inducing autophagy [39,40,42], we wanted to examine how knocking out ATG13 would affect the development of lipid droplets after glutamine metabolism blockade. As expected, the quantity of lipid droplets was remarkably reduced in cells with low expression of ATG13 despite being unable to access glutamine, suggesting that autophagy is required to accumulate PUFAs and lipid droplets (Fig. 2F). These results underscore the necessity of autophagy for managing lipid metabolism and highlight the interplay between glutamine metabolism and autophagic processes in HNSCC.

Lipid droplet biogenesis can play a protective role in cells by maintaining mitochondrial function during starvation-induced autophagy [38]. To explore whether glutamine blockade affects the function of the mitochondria, we performed a Seahorse Metabolic Stress test. The Seahorse assay results further illustrate this interplay: cells treated with DON exhibited significantly reduced basal oxygen consumption rate (OCR) (Supplemental Fig. 3D right panel), compared to untreated cells but showed a marked increase in maximal OCR upon carbonyl cyanide-4-(trifluoromethoxy)phenylhydrazone (FCCP) treatment (Supplemental Fig. 3D bottom panel). Glutamine antagonism may reduce substrate availability for the TCA cycle, leading to lower basal mitochondrial respiration observed. However, while glutamine antagonism initially suppresses mitochondrial respiration, it may prime the cells to exhibit a heightened respiratory capacity under uncoupled conditions, likely due to the reported adaptive mitochondrial responses initiated by autophagy and lipid biogenesis [38]. The extracellular acidification rate (ECAR), which measures the conversion of glucose to lactate, Supplemental Fig. 3E showed that ECAR was decreased at all metabolic stress points.

#### 4.3. Genome-wide CRISPR/Cas9 screen reveals the interaction of PUFA metabolism with glutamine metabolism blockade and identifies novel synthetic lethal targets

To profile the effect of glutamine metabolism antagonism on the genetic interactome, we performed a genome-wide CRISPR knock-out screen in HNSCC in the context of glutamine metabolism blockade (Fig. 3A). Using Cas9-expressing CAL33 HNSCC cells infected with the Brunello Human Genome pooled sgRNA library, cells were passaged under 0.25  $\mu$ M DON or vehicle for 18 cell doublings (Fig. 3A right panel). To evaluate pathways that, when modulated, resulted in resistance to glutamine metabolism inhibition, we examined sgRNAs enriched in the DON treatment condition (Fig. 3B). Aligned with the metabolomic analysis, the top hits were genes involved in alpha-linolenic acid and linoleic acid KEGG pathways, suggesting that reduced PUFA metabolism could drive resistance to glutamine metabolism blockade (Fig. 3C). We also observed the enrichment of cells with SOD1 and CYP2E1 in the DON treatment condition (Fig. 3D), which are regulators of the peroxisome pathway [42,43] that converts superoxide ( $O_2^-$ ) to hydrogen peroxide ( $H_2O_2$ ). Aligned with this, we observed a depletion of sgRNAs for antioxidant enzymes IDH1 and GPX4 (Fig. 3D), which play crucial cellular defense roles against oxidative stress and lipid peroxidation [44,45].

The CRISPR knock-out screen revealed PUFA metabolism and peroxidation genes as resistor genes, while antioxidant enzymes sensitize to glutamine metabolism blockade. This raises the possibility of a link between glutamine metabolism antagonism and the accumulation of lipid peroxides, a hallmark of iron-dependent cell death, ferroptosis [46]. Further delineation of the sgRNA targeting genes for critical players in the ferroptosis pathways (e.g., GPX4, FTL, GSS, STEAP3, and others) strengthened our hypothesis that glutamine metabolism blockade can sensitize HNSCC cells to lipid peroxidation (Fig. 3 D, E).

#### 4.4. Glutamine metabolism blockade leads to the accumulation of ROS and sensitizes cells to ferroptosis

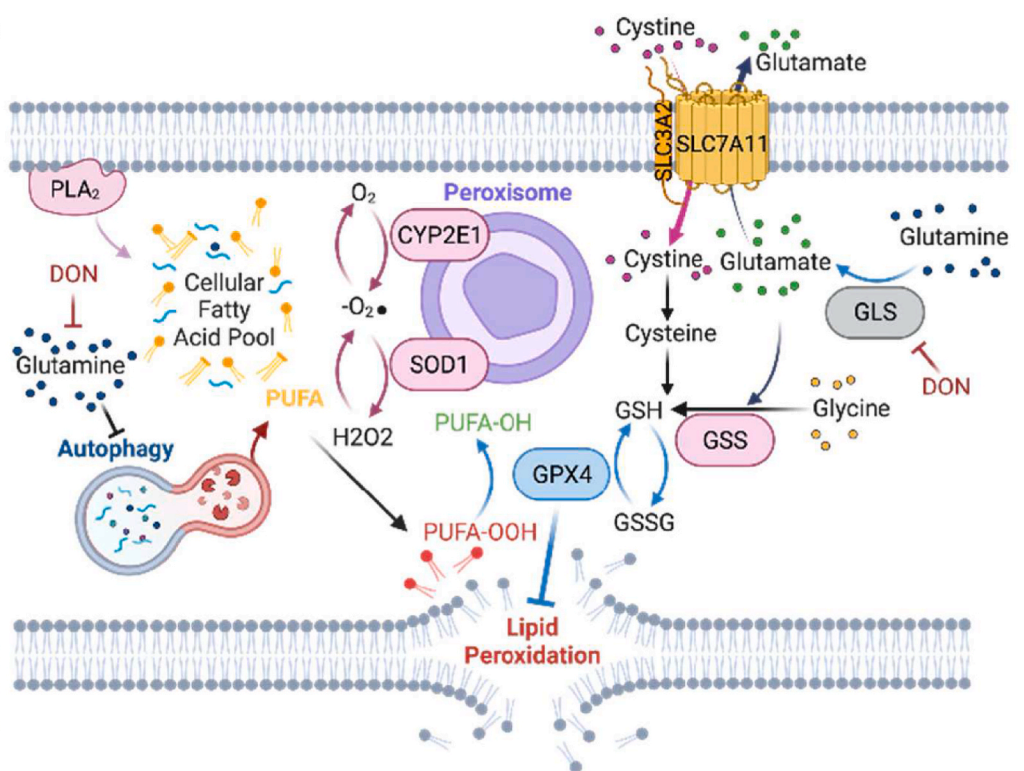
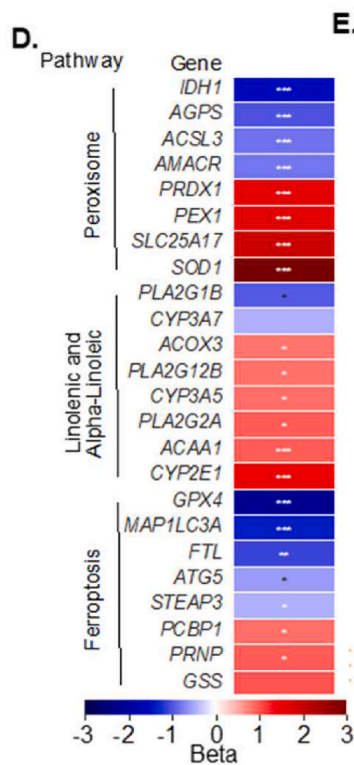
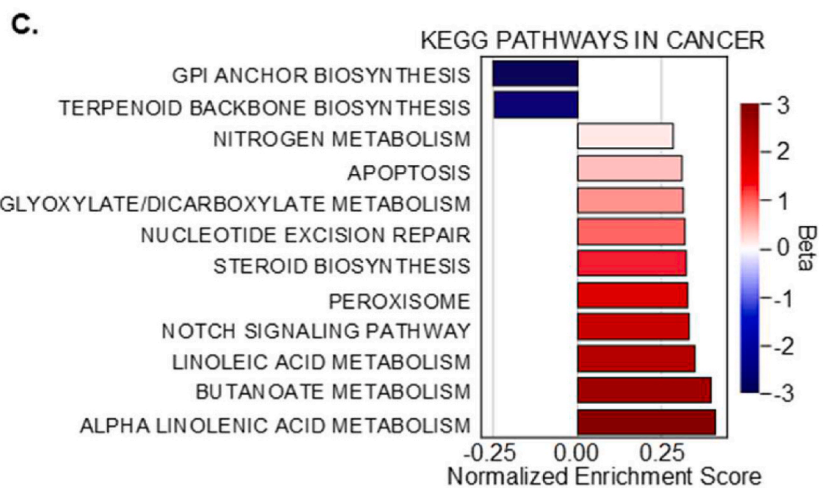
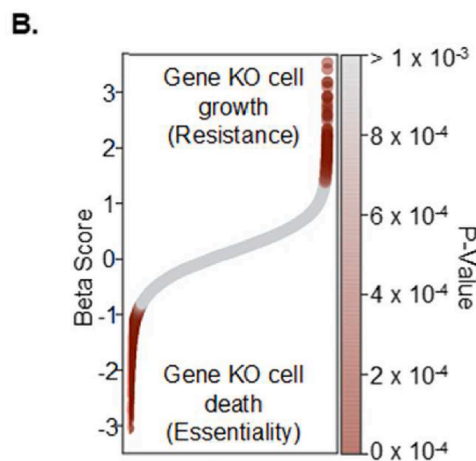
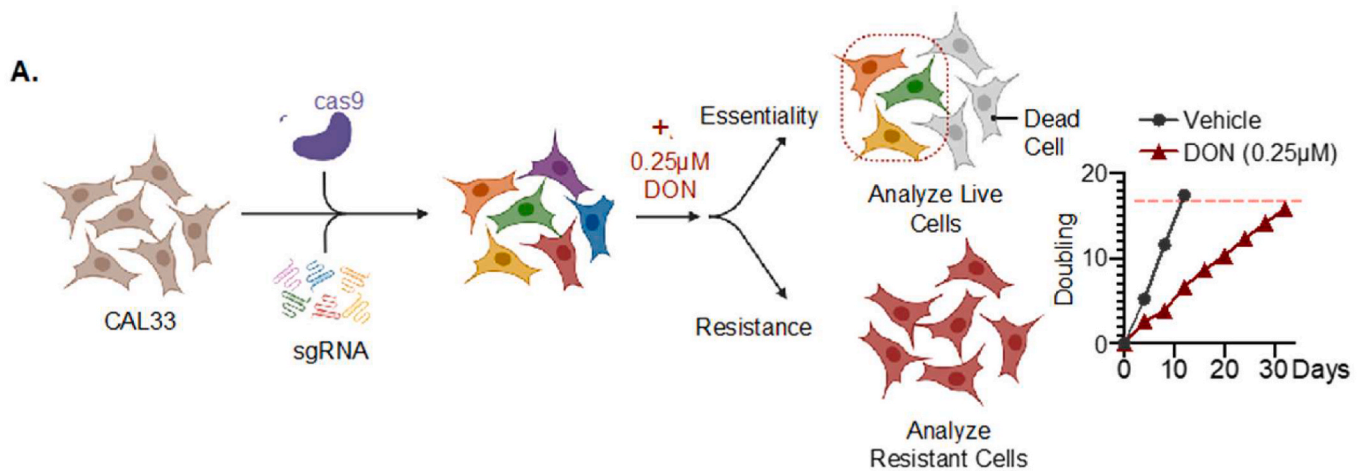
To validate our screen, we performed siRNA-mediated knockdown of essential genes sensitizing to ferroptosis (GPX4 and FTL) and fatty acid biosynthesis (ACLY) to evaluate the effect on live cell number with glutamine metabolism inhibition. As anticipated, the knockdown of GPX4 and FTL significantly increased sensitivity to glutamine metabolism antagonism (Fig. 4A). GPX4, a critical defense against ferroptosis, is notably vulnerable to inhibition in therapy-resistant tumors [46]. We observed a synergistic interaction between GPX4 knockdown and DON using the  $\Delta$ Bliss model to assess drug interactions (Fig. 4A). Both CAL27 and CAL33 cells in-vivo and in-vitro exhibited increased GPX4 expression upon DON treatment, potentially as a cellular response to mitigate oxidative degradation of PUFAs (Fig. 4B and Supplemental Figs. 5B–C). Additionally, glutathione (GSH) and its oxidized form (GSSG) levels were significantly decreased following DON treatment (Supplemental Fig. 3C). To further investigate the impact of reduced antioxidants due to glutamine antagonism on cellular reactive oxygen species (ROS) homeostasis, we measured  $H_2O_2$  levels and the oxidation of DCFH, which produces green-fluorescent molecules (Fig. 4C and D and Supplemental Figs. 4A–B). DON treatment led to elevated hydrogen peroxide levels (Fig. 4C) and increased oxidation of the ROS-probe DCFH in CAL33 and CAL27 cells (Fig. 4D, Supplemental Figs. 4A–B). These findings are aligned with our CRISPR screen data, which suggests that the peroxisome as a significant source of  $H_2O_2$  and a contributor to resistance against glutamine antagonism.

In light of these findings, we sought to explore whether blocking glutamine metabolism could sensitize cells to ferroptosis. To investigate this, cells were treated with escalating concentrations of DON and the ferroptosis activator RSL3 [45–47]. Synergistic antiproliferative effects were observed across multiple HNSCC cell lines (HPV- and HPV+), supporting a general drug-drug class pharmacodynamic interaction (Fig. 4G). In addition, HNSCC cells co-treated with escalating doses of DON and other ferroptosis inducers, such as erastin and imidazole-ketone-erastin (IKE), also showed synergy, albeit to a lesser extent than with RSL3 (Supplemental Fig. 5E).

As glutamine blockade sensitized cells to ferroptosis, we wanted to determine how supplementation of essential nutrients regulated ferroptosis induction. To explore the interplay between glutamine and glucose in ferroptosis, we assessed the response to RSL3 in cells incubated with different concentrations of these nutrients. We found that higher concentrations of both glutamine and glucose resulted in decreased sensitivity to RSL3 in HNSCC cells (Supplemental Fig. 4D and Supplemental Fig. 5A), suggesting that both nutrients can protect cells from ferroptosis, possibly via increased antioxidants from either the glutathione (glutamine) or pentose phosphate (glucose) pathways.

In contrast, supplementation with polyunsaturated fatty acids (e.g., linoleic acid), which were found to be increased upon glutamine blockade, potentiated HNSCC cell sensitivity to DON, RSL3, or combinatory treatment (RSL3+DON). We observed synergistic activity of linoleic acid with RSL3+DON, suggesting that dysregulation of PUFA metabolism can contribute to increased sensitivity to ferroptosis when cells do not have access to glutamine (Supplemental Fig. 4E). Interestingly, the DON and RSL3 administration sequence significantly influenced the cells' susceptibility to ferroptosis (Supplemental Fig. 5D). Specifically, cells treated first with DON for 24 h before RSL3 exhibited increased resistance to ferroptosis, suggesting that the induced upregulation of GPX4 by DON may provide cells with a means to escape ferroptosis.

To further elucidate how DON affected the growth of HNSCC cells, we incubated drug-treated cells with inhibitors of cell death pathways (e.g., apoptosis, ferroptosis, and necroptosis). As expected, concomitant treatment of RSL3 and the synthetic antioxidant ferrostatin-1 abolished RSL3's deleterious effect, serving as a control (Supplemental Fig. 4F). Conversely, we observed no reduction in DON's anti-proliferative effect



(caption on next page)

**Fig. 3. A genome-wide CRISPR/Cas9 screen reveals synthetic lethal and resistance interactors of glutamine metabolism antagonism.** **A.** CAL33 HNSCC cells expressing Cas9 were infected with the Brunello Human CRISPR sgRNA KO library at an MOI of 0.5. After selection, cells were treated with vehicle or 0.25  $\mu\text{M}$  of DON until cells doubled roughly 18 times, as displayed on the right. **B.** Beta scores for all tested genes are shown ordered by score. Genes found to be significantly enriched or depleted are colored in shades of red based on their p-value. **C.** Normalized enrichment scores of top 10 enriched, and all depleted KEGG pathways in MsigDB as measured by single-sample GSEA. **D.** Left, top genes of interacting KEGG pathways. Beta scores represent either essential (blue) or resistant (red) genes under DON treatment. Asterisks indicate significance; \* $p < 0.05$ , \*\* $p < 0.01$ , and \*\*\* $p < 0.001$ . **E.** Graphical model depicting the interaction of peroxisome, linolenic and alpha-linolenic metabolism, and ferroptosis. PLA2 catalyzes the release of polyunsaturated fatty acids, which are metabolized by CYP2E1 into substrates for lipid peroxidation. Hydrogen peroxide produced by SOD1 can be converted into highly reactive hydroxyl radicals, enhancing lipid peroxidation and ferroptosis. This process is delicately regulated by GPX4, which uses glutathione, derived from cysteine, glycine, and glutamate, to neutralize lipid peroxides. Any imbalance in these interconnected processes can tip the scale towards ferroptosis. Essential (blue) or resistant (red) genes are highlighted by color.

when combined with any cell death pathway inhibitor, indicating that DON does not induce cell death through these pathways. However, in cells treated with both DON and RSL3, ferrostatin and the apoptosis inhibitor (z-VAD-FMK) significantly increased live cell numbers, suggesting that the observed synergy involves both apoptosis and ferroptosis pathways (Supplemental Fig. 4F).

To explore whether DON treatment reduces cell proliferation rather than activating a cell-death pathway, we performed a MultiTox-Glo Assay, which sequentially measures both live-cell protease activity (indicating cell viability) and dead-cell protease activity (indicating cytotoxicity). Cells treated with DON and RSL3 had decreased cell numbers (Supplemental Fig. 4G), but when compared to cytotoxic cell death, RSL3-treated cells had high levels of the dead-cells, in contrast to DON-treated cells, suggesting that DON reduces proliferation rather than increasing cell death (Supplemental Fig. 4H).

#### 4.5. Glutamine metabolism antagonism increases the response to GPX4 inhibition in xenograft HNSCC mouse models

Based on our findings, we then used HNSCC xenograft models to evaluate the anticancer activity of the DON-prodrug DRP-104 and RSL3 combination *in vivo*. SCID/NSG mice were injected subcutaneously with HNSCC cell lines (CAL27 and CAL33) and randomly divided into four groups: Vehicle, RSL3, DRP-104, and RSL3+DRP-104. Mice were injected intratumorally with 100 mg/kg of RSL3 twice weekly for two weeks, as described previously [45]. DRP-104 was administered subcutaneously 5 days per week. Contrary to what we observed *in-vitro*, treatment with RSL3 alone *in-vivo* did not reduce tumor growth or tumor weight (Fig. 5A and Supplemental Fig. 6A). However, when combined with DRP-104, we observed a significant reduction in tumor volume and weight compared with the vehicle-treated control group and DRP-104 as a monotherapy (Fig. 5A). The observed rapid drop in tumor volume when using the combination of DRP-104 and RSL3 versus DRP-104 alone is still not fully understood and can likely reflect the synergistic action of these drugs. For instance, RSL3 action upon GPX4 inhibition may be more potent when glutamine metabolism is simultaneously hampered by DRP-104, leading to a faster and more potent onset of ferroptosis and the consequent rapid reduction in tumor volume. While these possibilities warrant further investigation, we evaluated the proliferation marker Ki67 in the HNSCC xenograft tumor specimens by IHC (Fig. 5B and Supplemental Fig. 6B).

We also evaluated the levels of 4-hydroxynonenal (4HNE), a marker of lipid peroxidation, in the tumor tissues [48]. The combination of DRP-104 and RSL3 led to a significant increase in 4HNE-positive cells compared to the vehicle and individual treatments (Fig. 5C). This increase in the lipid peroxidation marker supports enhanced ferroptosis observed with the combination treatment. Taken together, these findings suggest a direct connection between repressed glutamine metabolism and ferroptosis through autophagy-mediated PUFA accumulation, increased  $\text{H}_2\text{O}_2$  and ROS levels, and reduction of protective antioxidant systems (Fig. 5D).

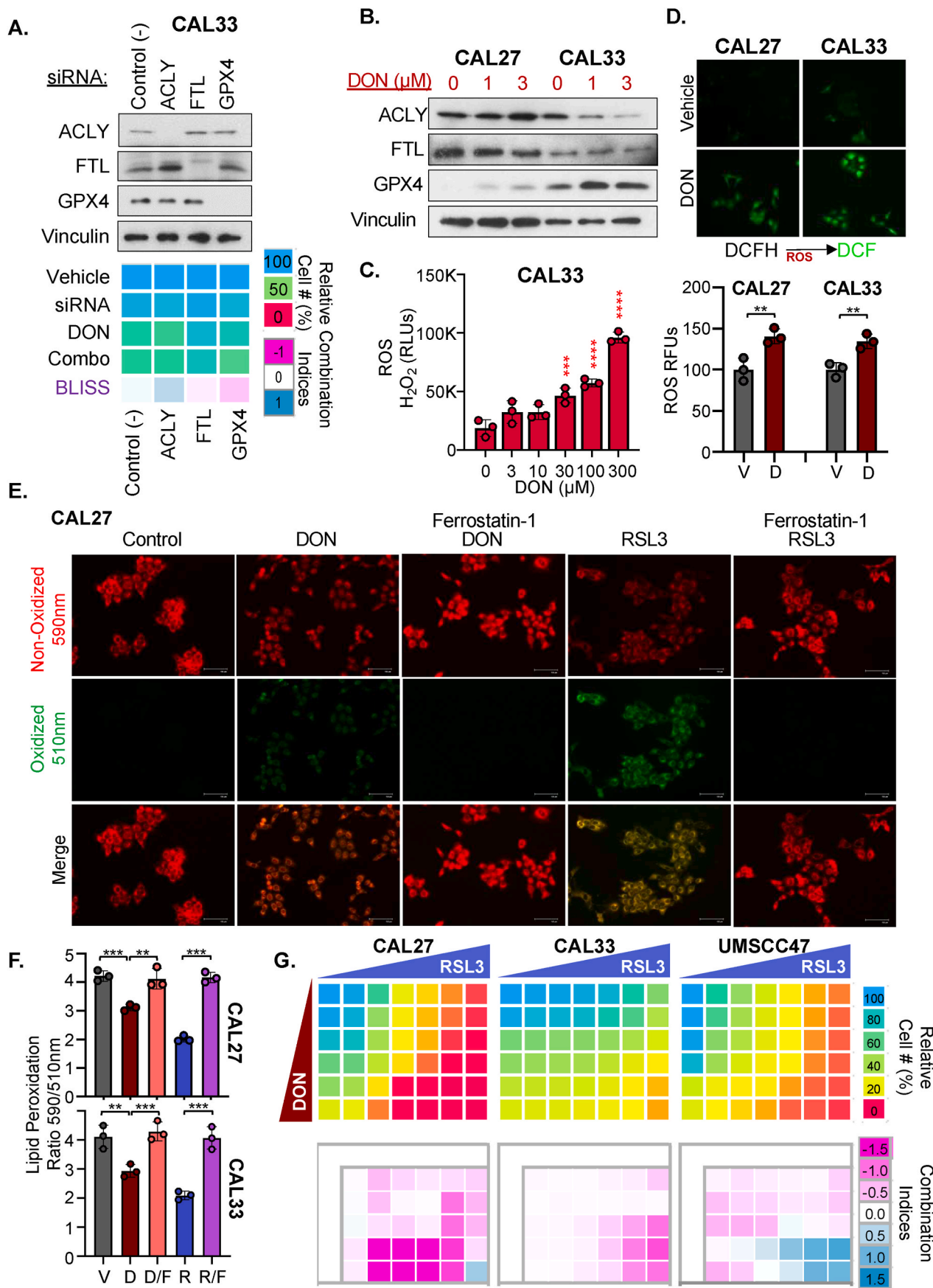
## 5. Discussion

Glutamine plays a significant role in the metabolism of highly

proliferating cells, including HNSCC [23]. Thus, a deep understanding of the shift in metabolic networks in response to glutamine deprivation may provide an opportunity to identify novel metabolism-based target therapies for HNSCC. However, targeting glutamine dependence through selective glutaminase antagonists, such as CB-839, although promising in pre-clinical studies, has been a disappointment in the clinic [27,49]. Presumably, inhibiting all known glutamine-metabolizing enzymes, rather than only glutaminase, with the glutamine analog DON would confer a better anti-tumor response. Our findings demonstrate that DON is an attractive therapeutic agent for preventing HNSCC tumor growth. We also observed that HNSCC cells carrying genetic alterations in the *PIK3CA/PTEN* pathway were more sensitive to glutamine metabolism antagonism than unaltered HNSCC cells. This increased sensitivity of HNSCC cells harboring *PIK3CA/PTEN* mutations could indicate a reliance on glutamine metabolism in these hyperactive mTOR signaling cells. While further work is required to elucidate the molecular basis of the increased dependence on glutamine metabolism, this sensitivity may be clinically relevant, as *PIK3CA* pathway hyperactivity is a frequent event in HNSCC [3], and its activation status can allow for further eligibility/stratification in future clinical trials.

Therapeutic opportunities targeting glutamine metabolism extend beyond HNSCC. Recent studies in preclinical models of pancreatic ductal adenocarcinoma (PDAC) using DRP-104 have highlighted the potential of this approach though tumors adapt and develop resistance through persistent MEK/ERK signaling, which can be counteracted with the MEK inhibitor trametinib [50]. A parallel study showed that DON triggers PDAC tumors to upregulate asparagine synthesis, rendering them vulnerable to asparaginase treatment [51]. These studies reinforce the therapeutic potential of targeting glutamine metabolism in cancer therapy and provide a mechanistic rationale for patient selection in future precision clinical trials and targeted options to overcome treatment resistance. In the case of HNSCC, our dissection of the metabolic network regulated by glutamine, using the glutamine analog DON, led to the finding that poly-unsaturated fatty acid metabolism is dysregulated upon glutamine metabolism blockade. Further interrogation into the underlying mechanism revealed that nutrient-sensing kinase mTOR is inhibited, leading to the activation of autophagy through ULK1-mediated phosphorylation of ATG13 at Ser-355. In addition, our CRISPR screen confirmed the convergence of PUFA and glutamine metabolism while identifying that the loss of pathways that play crucial cellular defense roles against oxidative stress and lipid peroxidation can sensitize HNSCC cells to glutamine metabolism blockade. Finally, we demonstrate that disruption of glutamine pathways using DON and its prodrug DRP-104 (sirpiglenastat) can significantly augment the sensitivity of HNSCC cells to ferroptosis activators. These findings revealed that glutamine metabolism blockade causes the rewiring of metabolic networks in cancer cells to fulfill their needs for nutrients and energy. This reprogramming exposes new metabolic liabilities, rendering them uniquely vulnerable to ferroptosis, which may present as a promising therapeutic option for patients with advanced and metastatic HNSCC, as well as for other human malignancies.

In this regard, while conducting these studies, we observed that the sequence of administration of DON and RSL3 influences the activation of ferroptosis, as their co-administration is synergistic, but pre-treatment with DON before RSL3 reduces the response. We can hypothesize that



(caption on next page)

**Fig. 4.** Antagonism of glutamine metabolism sensitizes cells to ferroptosis. CAL33 cells were treated with siRNAs targeting ACLY, FTL, or GPX4 and subsequently with 3  $\mu$ M DON for 24 h, followed by measurement of live cell number and determination of combination indices using  $\Delta$ BLISS (score <0 indicates synergism, score = 0 indicates additivity, score >0 indicates antagonism, scale from -1 to +1) (A). CAL27 and CAL33 cells were treated with increasing concentrations of DON (0, 1, 3  $\mu$ M) and analyzed by Western blot for levels of ACLY, FTL, and GPX4 (B). ROS levels in CAL33 cells were measured using H<sub>2</sub>O<sub>2</sub> substrate dilution buffer, and luminescence was recorded after 6 h of treatment, showing significant increases in ROS levels with higher concentrations of DON (C). ROS levels were also measured using DCFH-DA in CAL27 and CAL33 cells treated with vehicle or 3  $\mu$ M DON, demonstrating increased ROS levels in DON-treated cells (D). Lipid peroxidation was analyzed in CAL27 cells treated with 3  $\mu$ M DON, ferrostatin-1 (1  $\mu$ M), and RSL3 (2  $\mu$ M), with cells stained for oxidized (510 nm) and non-oxidized (590 nm) lipids (E). Quantification of the lipid peroxidation ratio (590/510 nm) in CAL27 and CAL33 cells treated with vehicle (V), 3  $\mu$ M DON (D), DON and ferrostatin-1 (D/F), or RSL3 and ferrostatin-1 (R/F) showed significant increases in lipid peroxidation with DON and RSL3 treatments (F). The viability of CAL27, CAL33, and UMSSC47 cells treated with various combinations of DON and RSL3 was assessed, with heatmap representation of live cell number and determination of combination indices using  $\Delta$ BLISS (scale from -2 to +2) (G). All data represent averages  $\pm$ SD, except where indicated. \**P* < 0.05, \*\**P* < 0.01, \*\*\**P* < 0.001, \*\*\*\**P* < 0.0001. Source data are provided as a Source Data file.

the adaptive induction of GPX4 expression by DON may provide cells with a means to escape ferroptosis. Indeed, the feedback upregulation of GPX4 suggests the existence of a therapeutic window during which cells are particularly vulnerable to ferroptosis following glutamine antagonism. This hypothesis is supported by previous studies showing that GPX4 expression can be increased by certain fatty acids, potentially enhancing cellular defense mechanisms against ferroptosis [52]. We also observed that specific HNSCC cells that express low levels of GPX4 (e.g., CAL27 and SCC47 cells) are more sensitive to RSL3, which suggests that their adaptation to low GPX4 may make them more sensitive to GPX4 inhibition by RSL3. These studies underscore the possibility of predicting treatment sensitivity by leveraging the balance between metabolic pathways and adaptive cellular defense processes for inducing ferroptosis. These findings also support the idea that fully elucidating the underlying mechanisms may enable the full exploitation of this vulnerability window.

While apoptosis evasion has been recognized as a hallmark of cancer, novel modes of cell death that are mechanistically and morphologically different from apoptosis and, therefore, hold great potential for cancer therapy have more recently come into focus. Ferroptosis is an iron-dependent form of regulated cell death triggered by the toxic build-up of lipid peroxides on cellular membranes [44,45]. Morphologically, this leads to the rupture of the mitochondrial outer membrane and cellular disintegration [44,45]. The most essential mitigator of ferroptosis is the selenoprotein glutathione peroxidase 4 (GPX4), which scavenges cellular ROS through glutathione (GSH) to convert lipid peroxides to non-toxic lipid alcohols, directly suppressing lipid peroxidation. Unfortunately, most GPX4 inhibitors have exhibited poor (or unclear) pharmacological properties in animal models, limiting their potential for clinical translation [53]. Therefore, several additional challenges remain to be addressed to realize the full potential of glutamine-based ferroptosis-inducing strategies. Here, we show that DON sensitizes cells to ferroptosis-inducing agents, such as RSL3, erastin and IKE, albeit the degree of synergy may vary depending on the specific inhibitor used. Mechanistically, this process may involve the adaptive response to glutamine metabolism inhibition, which results in the accumulation of PUFAs that are direct substrates of peroxidizing enzymes. In turn, this suggests that the future development of ferroptosis-inducing agents could benefit from exploring synergistic combinations, such as upon glutamine metabolism inhibition in HNSCC cancer cells and yet-to-be-identified sensitizing mechanisms in other cancer types, thus increasing the effectiveness of ferroptosis-based therapies while limiting their toxicities.

In addition to cancer cells, immune cells that promote or suppress antitumor immunity might also be susceptible to glutamine metabolism antagonism and ferroptosis. Therefore, balancing the glutamine blockade-induced ferroptosis vulnerabilities of cancer cells, antitumor immune cells, and immunosuppressive cells represents an exciting area of future investigation. In this regard, it has been recently shown that DON shuts down glycolysis and oxidative phosphorylation in mouse cancer cells while enhancing T cell oxidative phosphorylation and anticancer immune responses [54]. In addition, targeting glutamine metabolism can modulate the tumor microenvironment by inhibiting

the recruitment of myeloid-derived suppressor cells [55]. Furthermore, DRP-104 increased activated T, NK, and NKT cell infiltration to tumors, polarized macrophages to M1 phenotype, increased CD103<sup>+</sup>DC, and demonstrated therapeutic synergy with multiple immune checkpoint inhibitor approaches in preclinical models [56]. This suggests that the comprehensive understanding of the mechanisms underlying the differential sensitivities of cancer cells and immune cells to glutamine metabolism inhibition may enable the development of suitable combinations with immune checkpoint-blocking therapies.

Glucose metabolism is crucial for HNSCC growth [16,20,21], and a metabolic shift from glucose to glutamine might occur under certain conditions, such as hypoxic stress [24,57]. As such, the dual inhibition of glutamine and glucose metabolism may represent a promising strategy worth investigating in future studies. In this regard, our current findings, in the context of a prior body of literature, underscore the complex relationship between glutamine metabolic networks and oxidative homeostasis in cancer. Indeed, pathways identified by our screen and metabolomics may represent compensatory mechanisms that converge to attempt to ensure survival when cancer cells do not have access to glutamine. Ultimately, glutamine metabolism blockade may induce a ferroptosis-sensitive state through multiple pathways that, when maximally unleashed, may be uniquely translated to potent, targeted ferroptosis combination therapies.

#### Additional information

This work was supported, in whole or in part, by R01DE026644 and R01DE026870 to JSG, Dracen Pharmaceuticals, and 28DT-0011 to DN. MMA was supported by a fellowship from the Howard Hughes Medical Institute Gilliam Fellowship. Dracen Pharmaceuticals provided DRP-104 (sirpiglenastat).

#### Ethics statement

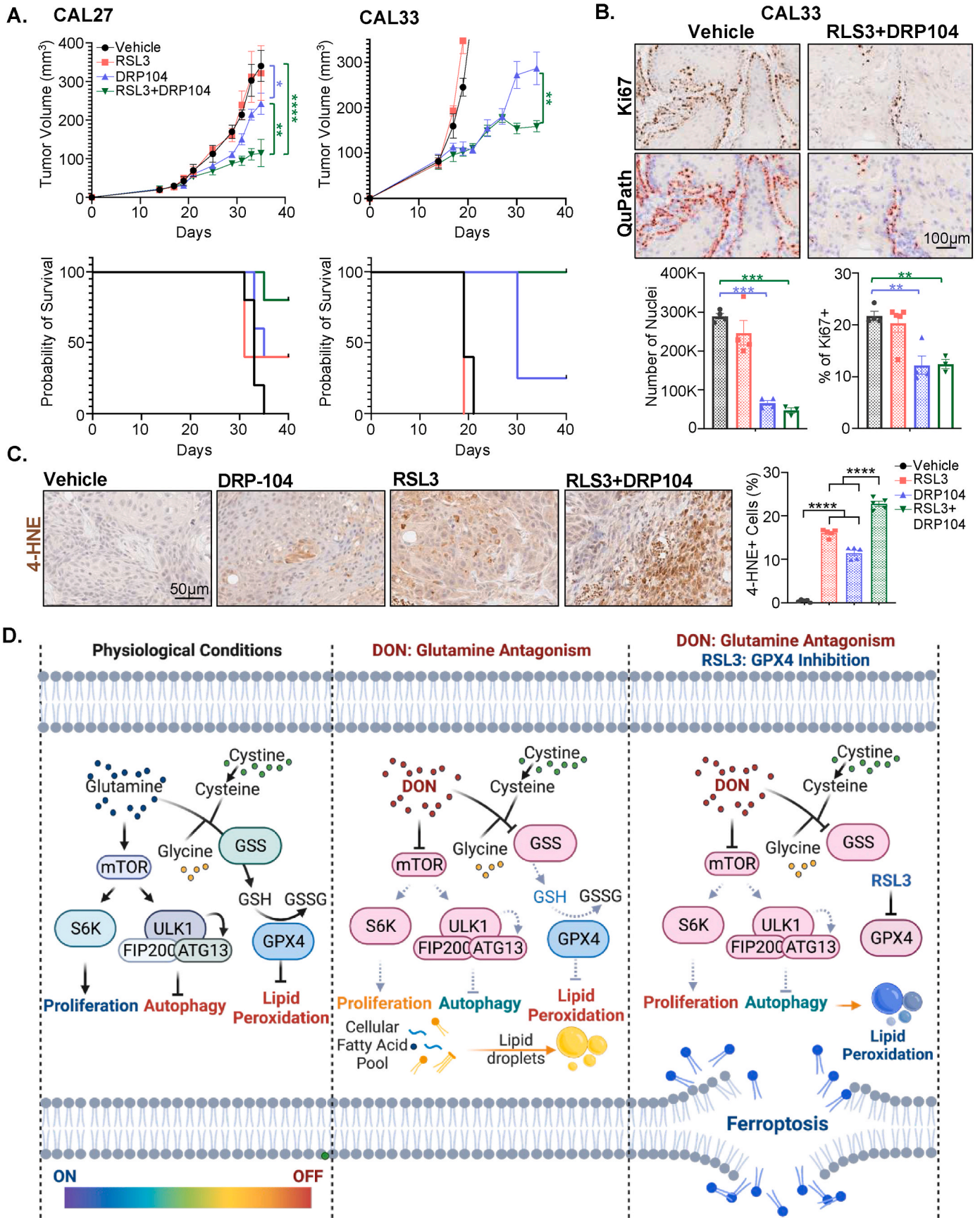
This manuscript represents the authors' original work and has not been previously published. All research was conducted truthfully, with meaningful contributions from all co-authors properly credited. The manuscript is not under simultaneous consideration elsewhere.

#### Animal studies

All animal experiments complied with the ARRIVE guidelines and were conducted by institutional guidelines, the U.K. Animals (Scientific Procedures) Act, 1986, and EU Directive 2010/63/EU. The care of animals followed institutional guidelines, and experimental protocols were approved by the Institutional Animal Care and Use Committee (IACUC) of the University of California, San Diego (Protocol Number: S15195).

#### Conflict of interest disclosure statement

Robert Wild and Yumi Yokoyama are stockholders of Dracen Pharmaceuticals. Robert Wild reports consulting fees from Dracen Pharmaceuticals. J. Silvio Gutkind reports consulting fees from Domain



(caption on next page)

**Fig. 5.** Glutamine metabolism blockade and ferroptosis activation reduce HNSCC tumor growth. **A.** CAL27 and CAL33 HNSCC cells were transplanted into NSG mice and treated subcutaneously with vehicle control diluent or DRP-104 (3 mg/kg) five times per week for four weeks. Mice were also treated intratumorally with four doses of RSL3 or vehicle diluent. Bottom, Kaplan-Meier survival curve representing the survival of the mice in each treatment group, with a cut-off at 250 mm (n = 5 mice per group). **B.** Top, Representative immunohistochemical analysis of proliferation marker Ki67. Middle, Ki67 positive or negative nuclei identified by QuPath cell detection tool. Bottom, quantification of total nuclei and percentage of Ki67 is displayed below. **C.** Immunohistochemical analysis of 4-HNE in CAL27 xenografts treated with vehicle, RSL3, DRP104, or the combination of RSL3 and DRP104, with quantification of 4-HNE positive cells presented. \*P < 0.05, \*\*P < 0.01, \*\*\*P < 0.001, \*\*\*\*P < 0.0001. **D.** Model depicting proliferative and physiological conditions (left), glutamine-inhibition (center), and enhanced ferroptosis induction of HNSCC cells (right). Highly proliferative cells in glutamine-rich environments engage regulator pathways to inhibit autophagy and prevent the formation of toxic lipid reactive oxygen species (ROS). Disruption of glutamine metabolism in HNSCC cells leads to the inhibition of mTOR and, subsequently, the accumulation of intracellular fatty acids through autophagy-mediated degradation of organelles. Augmented levels of polyunsaturated fatty acids and reductions of the anti-oxidant glutathione due to glutamine blockade sensitize HNSCC cells for ferroptosis-induction via RSL3.

Pharmaceuticals, Pangea Therapeutics, and io9 and is the founder of Kadima Pharmaceuticals, all unrelated to the current study. Daniela Nachmanson is an employee of TwinStrand Biosciences. Olivier Harismendy is a current employee and shareholder of Zentalis Pharmaceuticals. All other authors declare no potential conflicts of interest.

#### CRediT authorship contribution statement

**Michael M. Allevato:** Writing – original draft, Methodology, Investigation, Formal analysis, Data curation, Conceptualization. **Sally Trinh:** Investigation. **Keiichi Koshizuka:** Investigation. **Daniela Nachmanson:** Resources, Methodology, Formal analysis, Data curation. **Thien-Tu C. Nguyen:** Investigation. **Yumi Yokoyama:** Investigation, Formal analysis. **Xingyu Wu:** Methodology, Investigation, Formal analysis. **Allen Andres:** Methodology, Investigation. **Zhiyong Wang:** Investigation, Formal analysis. **Jeremie Watrous:** Investigation. **Alfredo A. Molinolo:** Validation, Investigation. **Prashant Mali:** Visualization, Supervision, Methodology. **Olivier Harismendy:** Methodology, Formal analysis, Data curation. **Mohit Jain:** Methodology, Investigation. **Robert Wild:** Writing – review & editing, Resources, Conceptualization. **J. Silvio Gutkind:** Writing – review & editing, Supervision, Resources, Project administration, Conceptualization.

#### Declaration of competing interest

The authors declare the following financial interests/personal relationships which may be considered as potential competing interests:

Robert Wild and Yumi Yokoyama are stockholders of Dracen Pharmaceuticals. Robert Wild reports consulting fees from Dracen Pharmaceuticals. J. Silvio Gutkind reports consulting fees from Domain Pharmaceuticals, Pangea Therapeutics, and io9 and is the founder of Kadima Pharmaceuticals, all unrelated to the current study. Daniela Nachmanson is an employee of TwinStrand Biosciences. Olivier Harismendy is a current employee and shareholder of Zentalis Pharmaceuticals. All other authors declare no potential conflicts of interest.

#### Appendix A. Supplementary data

Supplementary data to this article can be found online at <https://doi.org/10.1016/j.canlet.2024.217089>.

#### References

- [1] R.L. Siegel, K.D. Miller, N.S. Wagle, A. Jemal, Cancer statistics, *CA Cancer J Clin* 73 (2023) (2023) 17–48.
- [2] D. Pulte, H. Brenner, Changes in survival in head and neck cancers in the late 20th and early 21st century: a period analysis, *Oncol.* 15 (2010) 994–1001.
- [3] R. Iglesias-Bartolome, D. Martin, J.S. Gutkind, Exploiting the head and neck cancer oncogenome: widespread PI3K-mTOR pathway alterations and novel molecular targets, *Cancer Discov.* 3 (2013) 722–725.
- [4] V.W. Lui, M.L. Hedberg, H. Li, B.S. Vangara, K. Pendleton, Y. Zeng, Y. Lu, Q. Zhang, Y. Du, B.R. Gilbert, M. Freilino, S. Sauerwein, N.D. Peyser, D. Xiao, B. Diergaarde, L. Wang, S. Chiosea, R. Seethala, J.T. Johnson, S. Kim, U. Duvvuri, R.L. Ferris, M. Romkes, T. Nukui, P. Kwok-Shing Ng, L.A. Garraway, P.S. Hammerman, G. B. Mills, J.R. Grandis, Frequent mutation of the PI3K pathway in head and neck cancer defines predictive biomarkers, *Cancer Discov.* 3 (2013) 761–769.
- [5] N. Cancer Genome Atlas, Comprehensive genomic characterization of head and neck squamous cell carcinomas, *Nature* 517 (2015) 576–582.
- [6] A.A. Molinolo, S.M. Hewitt, P. Amornphimoltham, S. Keelawat, S. Rangdaeng, A. Meneses Garcia, A.R. Raimondi, R. Jufe, M. Itoiz, Y. Gao, D. Saranath, G. S. Kaleebi, G.H. Yoo, L. Leak, E.M. Myers, S. Shintani, D. Wong, H.D. Massey, W. A. Yeudall, F. Lonardo, J. Ensley, J.S. Gutkind, Dissecting the Akt/mammalian target of rapamycin signaling network: emerging results from the head and neck cancer tissue array initiative, *Clin. Cancer Res.* 13 (2007) 4964–4973.
- [7] A.A. Molinolo, C. Marsh, M. El Dinali, N. Gangane, K. Jennison, S. Hewitt, V. Patel, T.Y. Seiwert, J.S. Gutkind, mTOR as a molecular target in HPV-associated oral and cervical squamous carcinomas, *Clin. Cancer Res.* 18 (2012) 2558–2568.
- [8] A.R. Raimondi, A. Molinolo, J.S. Gutkind, Rapamycin prevents early onset of tumorigenesis in an oral-specific K-ras and p53 two-hit carcinogenesis model, *Cancer Res.* 69 (2009) 4159–4166.
- [9] R. Czerninski, P. Amornphimoltham, V. Patel, A.A. Molinolo, J.S. Gutkind, Targeting mammalian target of rapamycin by rapamycin prevents tumor progression in an oral-specific chemical carcinogenesis model, *Cancer Prev. Res.* 2 (2009) 27–36.
- [10] V. Patel, C.A. Marsh, R.T. Dorsam, C.M. Mikelis, A. Masedunskas, P. Amornphimoltham, C.A. Nathan, B. Singh, R. Weigert, A.A. Molinolo, J. S. Gutkind, Decreased lymphangiogenesis and lymph node metastasis by mTOR inhibition in head and neck cancer, *Cancer Res.* 71 (2011) 7103–7112.
- [11] K. Saito, S. Matsumoto, H. Yasui, N. Devasahayam, S. Subramanian, J. P. Munasinghe, V. Patel, J.S. Gutkind, J.B. Mitchell, M.C. Krishna, Longitudinal imaging studies of tumor microenvironment in mice treated with the mTOR inhibitor rapamycin, *PLoS One* 7 (2012) e49456.
- [12] C.H. Squarize, R.M. Castilho, J.S. Gutkind, Chemoprevention and treatment of experimental Cowden's disease by mTOR inhibition with rapamycin, *Cancer Res.* 68 (2008) 7066–7072.
- [13] Z.J. Sun, L. Zhang, B. Hall, Y. Bian, J.S. Gutkind, A.B. Kulkarni, Chemopreventive and chemotherapeutic actions of mTOR inhibitor in genetically defined head and neck squamous cell carcinoma mouse model, *Clin. Cancer Res.* 18 (2012) 5304–5313.
- [14] T.A. Day, K. Shirai, P.E. O'Brien, M.G. Matheus, K. Godwin, A.J. Sood, A. Kompelli, J.A. Vick, D. Martin, L. Vitale-Cross, J.L. Callejas-Varela, Z. Wang, X. Wu, O. Harismendy, A.A. Molinolo, S.M. Lippman, C. Van Waes, E. Szabo, J.S. Gutkind, Inhibition of mTOR signaling and clinical activity of rapamycin in head and neck cancer in a window of opportunity trial, *Clin. Cancer Res.* 25 (2019) 1156–1164.
- [15] E.E. Cohen, K. Wu, C. Hartford, M. Kocherginsky, K.N. Eaton, Y. Zha, A. Nallari, M. L. Maitland, K. Fox-Kay, K. Moshier, L. House, J. Ramirez, S.D. Undevia, G. F. Fleming, T.F. Gajewski, M.J. Ratain, Phase I studies of sirolimus alone or in combination with pharmacokinetic modulators in advanced cancer patients, *Clin. Cancer Res.* 18 (2012) 4785–4793.
- [16] R.A. Cairns, I.S. Harris, T.W. Mak, Regulation of cancer cell metabolism, *Nat. Rev. Cancer* 11 (2011) 85–95.
- [17] D. Hanahan, R.A. Weinberg, Hallmarks of cancer: the next generation, *Cell* 144 (2011) 646–674.
- [18] O. Warburg, On the origin of cancer cells, *Science* 123 (1956) 309–314.
- [19] L.M. Ferreira, Cancer metabolism: the Warburg effect today, *Exp. Mol. Pathol.* 89 (2010) 372–380.
- [20] D.R. Wise, R.J. DeBerardinis, A. Mancuso, N. Sayed, X.Y. Zhang, H.K. Pfeiffer, I. Nissim, E. Daikhin, M. Yudkoff, S.B. McMahon, C.B. Thompson, Myc regulates a transcriptional program that stimulates mitochondrial glutaminolysis and leads to glutamine addiction, *Proc Natl Acad Sci U S A* 105 (2008) 18782–18787.
- [21] C. Yang, J. Sudderth, T. Dang, R.M. Bachoo, J.G. McDonald, R.J. DeBerardinis, Glioblastoma cells require glutamate dehydrogenase to survive impairments of glucose metabolism or Akt signaling, *Cancer Res.* 69 (2009) 7986–7993.
- [22] R.J. DeBerardinis, A. Mancuso, E. Daikhin, I. Nissim, M. Yudkoff, S. Wehrli, C. B. Thompson, Beyond aerobic glycolysis: transformed cells can engage in glutamine metabolism that exceeds the requirement for protein and nucleotide synthesis, *Proc Natl Acad Sci U S A* 104 (2007) 19345–19350.
- [23] P. Kamarajan, T.M. Rajendiran, J. Kinchen, M. Bermudez, T. Danciu, Y.L. Kapila, Head and neck squamous cell carcinoma metabolism Draws on glutaminolysis, and Stemness is specifically regulated by glutaminolysis via Aldehyde dehydrogenase, *J. Proteome Res.* 16 (2017) 1315–1326.
- [24] B.J. Altman, Z.E. Stine, C.V. Dang, From Krebs to clinic: glutamine metabolism to cancer therapy, *Nat. Rev. Cancer* 16 (2016) 749.
- [25] K.M. Lemberg, J.J. Vornov, R. Rais, B.S. Slusher, We're not "DON" yet: Optimal dosing and prodrug Delivery of 6-Diazo-5-oxo-L-norleucine, *Mol Cancer Ther* 17 (2018) 1824–1832.

- [26] C.A. Wicker, B.G. Hunt, S. Krishnan, K. Aziz, S. Parajuli, S. Palackdharry, W. R. Elaban, T.M. Wise-Draper, G.B. Mills, S.E. Waltz, V. Takiar, Glutaminase inhibition with telaglenastat (CB-839) improves treatment response in combination with ionizing radiation in head and neck squamous cell carcinoma models, *Cancer Lett.* 502 (2021) 180–188.
- [27] F. Skoulidis, J.W. Neal, W.L. Akerley, P.K. Paik, T. Papagiannakopoulos, K. L. Reckamp, J.W. Riess, Y. Jenkins, S. Holland, F. Parlari, Y. Shen, S.H. Whiting, N. A. Rizvi, A phase II randomized study of telaglenastat, a glutaminase (GLS) inhibitor, versus placebo, in combination with pembrolizumab (Pembro) and chemotherapy as first-line treatment for KEAP1/NRF2-mutated non-squamous metastatic non-small cell lung cancer (mNSCLC), *J. Clin. Oncol.* 38 (2020) TPS9627. TPS9627.
- [28] D.E. Biancur, J.A. Paulo, B. Malachowska, M. Quiles Del Rey, C.M. Sousa, X. Wang, A.S.W. Sohn, G.C. Chu, S.P. Gygi, J.W. Harper, W. Fendler, J.D. Mancias, A. C. Kimmelman, Compensatory metabolic networks in pancreatic cancers upon perturbation of glutamine metabolism, *Nat. Commun.* 8 (2017) 15965.
- [29] A.G. Thomas, C. Rojas, C. Tanega, M. Shen, A. Simeonov, M.B. Boxer, D.S. Auld, D. V. Ferraris, T. Tsukamoto, B.S. Slusher, Kinetic characterization of ebselen, chelerythrine and apomorphine as glutaminase inhibitors, *Biochem. Biophys. Res. Commun.* 438 (2013) 243–248.
- [30] R.T. Eagan, S. Frytak, W.C. Nichols, E.T. Creagan, J.N. Ingle, Phase II study on DON in patients with previously treated advanced lung cancer, *Cancer Treat Rep.* 66 (1982) 1665–1666.
- [31] R.H. Earhart, D.J. Amato, A.Y. Chang, E.C. Borden, M. Shiraki, M.E. Dowd, R. L. Comis, T.E. Davis, T.J. Smith, Phase II trial of 6-diazo-5-oxo-L-norleucine versus aclacinomycin-A in advanced sarcomas and mesotheliomas, *Invest New Drugs* 8 (1990) 113–119.
- [32] G. Lynch, N. Kemeny, E. Casper, Phase II evaluation of DON (6-diazo-5-oxo-L-norleucine) in patients with advanced colorectal carcinoma, *Am. J. Clin. Oncol.* 5 (1982) 541–543.
- [33] J. Rubin, S. Sorensen, A.J. Schutt, G.A. van Hazel, M.J. O’Connell, C.G. Moertel, A phase II study of 6-diazo-5-oxo-L-norleucine (DON, NSC-7365) in advanced large bowel carcinoma, *Am. J. Clin. Oncol.* 6 (1983) 325–326.
- [34] R. Rais, K.M. Lemberg, L. Tenora, M.L. Arwood, A. Pal, J. Alt, Y. Wu, J. Lam, J.M. H. Aguilar, L. Zhao, D.E. Peters, C. Tallon, R. Pandey, A.G. Thomas, R.P. Dash, T. Seiwert, P. Majer, R.D. Leone, J.D. Powell, B.S. Slusher, Discovery of DRP-104, a tumor-targeted metabolic inhibitor prodrug, *Sci. Adv.* 8 (2022) eabq5925.
- [35] Z. Wang, Y. Goto, M.M. Allevato, V.H. Wu, R. Saddawi-Konefka, M. Gilardi, D. Alvarado, B.S. Yung, A. O’Farrell, A.A. Molinolo, U. Duvvuri, J.R. Grandis, J. A. Califano, E.E.W. Cohen, J.S. Gutkind, Disruption of the HER3-PI3K-mTOR oncogenic signaling axis and PD-1 blockade as a multimodal precision immunotherapy in head and neck cancer, *Nat. Commun.* 12 (2021) 2383.
- [36] J.D. Watrous, T.J. Niiranen, K.A. Lagerborg, M. Henglin, Y.J. Xu, J. Rong, S. Sharma, R.S. Vasani, M.G. Larson, A. Armando, S. Mora, O. Quehenberger, E. A. Dennis, S. Cheng, M. Jain, Directed non-targeted mass spectrometry and chemical networking for Discovery of eicosanoids and related Oxylipins, *Cell Chem. Biol.* 26 (2019) 433–442 e434.
- [37] T. Pluskal, S. Castillo, A. Villar-Briones, M. Oresic, MZmine 2: modular framework for processing, visualizing, and analyzing mass spectrometry-based molecular profile data, *BMC Bioinf.* 11 (2010) 395.
- [38] T.B. Nguyen, S.M. Louie, J.R. Daniele, Q. Tran, A. Dillin, R. Zoncu, D.K. Nomura, J. A. Olzmann, DGAT1-Dependent lipid droplet biogenesis protects mitochondrial function during starvation-induced autophagy, *Dev. Cell* 42 (2017) 9–21 e25.
- [39] K.J. Petherick, O.J. Conway, C. Mpamhanga, S.A. Osborne, A. Kamal, B. Saxty, I. G. Ganley, Pharmacological inhibition of ULK1 kinase blocks mammalian target of rapamycin (mTOR)-dependent autophagy, *J. Biol. Chem.* 290 (2015) 28726.
- [40] R. Zoncu, A. Efeyan, D.M. Sabatini, mTOR: from growth signal integration to cancer, diabetes and ageing, *Nat. Rev. Mol. Cell Biol.* 12 (2011) 21–35.
- [41] K. Inoki, J. Kim, K.L. Guan, AMPK and mTOR in cellular energy homeostasis and drug targets, *Annu. Rev. Pharmacol. Toxicol.* 52 (2012) 381–400.
- [42] J. Xu, X. Su, S.K. Burley, X.F.S. Zheng, Nuclear SOD1 in growth control, oxidative stress response, Amyotrophic Lateral Sclerosis, and cancer, *Antioxidants* 11 (2022).
- [43] Y. Lu, A.I. Cederbaum, CYP2E1 and oxidative liver injury by alcohol, *Free Radic. Biol. Med.* 44 (2008) 723–738.
- [44] R.J. Molenaar, J.P. Maciejewski, J.W. Wilmink, C.J.F. van Noorden, Correction: Wild-type and mutated IDH1/2 enzymes and therapy responses, *Oncogene* 37 (2018) 5810.
- [45] W.S. Yang, R. SriRamaratnam, M.E. Welsch, K. Shimada, R. Skouta, V. S. Viswanathan, J.H. Cheah, P.A. Clemons, A.F. Shamji, C.B. Clish, L.M. Brown, A. W. Girotti, V.W. Cornish, S.L. Schreiber, B.R. Stockwell, Regulation of ferroptotic cancer cell death by GPX4, *Cell* 156 (2014) 317–331.
- [46] V.S. Viswanathan, M.J. Ryan, H.D. Dhruv, S. Gill, O.M. Eichhoff, B. Seashore-Ludlow, S.D. Kaffenberger, J.K. Eaton, K. Shimada, A.J. Aguirre, S.R. Viswanathan, S. Chattopadhyay, P. Tamayo, W.S. Yang, M.G. Rees, S. Chen, Z.V. Boskovic, S. Javaid, C. Huang, X. Wu, Y.Y. Tseng, E.M. Roeder, D. Gao, J.M. Cleary, B. M. Wolpin, J.P. Mesirov, D.A. Haber, J.A. Engelman, J.S. Boehm, J.D. Kotz, C. S. Hon, Y. Chen, W.C. Hahn, M.P. Levesque, J.G. Doench, M.E. Berens, A.F. Shamji, P.A. Clemons, B.R. Stockwell, S.L. Schreiber, Dependency of a therapy-resistant state of cancer cells on a lipid peroxidase pathway, *Nature* 547 (2017) 453–457.
- [47] M.J. Hangauer, V.S. Viswanathan, M.J. Ryan, D. Bole, J.K. Eaton, A. Matov, J. Galeas, H.D. Dhruv, M.E. Berens, S.L. Schreiber, F. McCormick, M.T. McManus, Drug-tolerant persister cancer cells are vulnerable to GPX4 inhibition, *Nature* 551 (2017) 247–250.
- [48] A. Benedetti, M. Comperti, H. Esterbauer, Identification of 4-hydroxynonenal as a cytotoxic product originating from the peroxidation of liver microsomal lipids, *Biochim. Biophys. Acta* 620 (1980) 281–296.
- [49] J.J. Harding, M.L. Telli, P.N. Munster, M.H. Le, C. Molineaux, M.K. Bennett, E. Mittra, H.A. Burris, A.S. Clark, M. Dunphy, F. Meric-Bernstam, M.R. Patel, A. DeMichele, J.R. Infante, Safety and tolerability of increasing doses of CB-839, a first-in-class, orally administered small molecule inhibitor of glutaminase, in solid tumors, *J. Clin. Oncol.* 33 (2015) 2512. 2512.
- [50] J. Encarnacion-Rosado, A.S.W. Sohn, D.E. Biancur, E.Y. Lin, V. Osorio-Vasquez, T. Rodrick, D. Gonzalez-Baerga, E. Zhao, Y. Yokoyama, D.M. Simeone, D.R. Jones, S.J. Parker, R. Wild, A.C. Kimmelman, Targeting pancreatic cancer metabolic dependencies through glutamine antagonism, *Nat Cancer* 5 (2024) 85–99.
- [51] M.V. Recouvreux, S.F. Grenier, Y. Zhang, E. Esparza, G. Lambies, C.M. Galapate, S. Maganti, K. Duong-Polk, D. Bhullar, R. Naeem, D.A. Scott, A.M. Lowy, H. Tiriach, C. Commisso, Glutamine mimicry suppresses tumor progression through asparagine metabolism in pancreatic ductal adenocarcinoma, *Nat Cancer* 5 (2024) 100–113.
- [52] A.A. Sneddon, H.C. Wu, A. Farquharson, I. Grant, J.R. Arthur, D. Rotondo, S. N. Choe, K.W. Wahle, Regulation of selenoprotein GPx4 expression and activity in human endothelial cells by fatty acids, cytokines and antioxidants, *Atherosclerosis* 171 (2003) 57–65.
- [53] J.K. Eaton, L. Furst, R.A. Ruberto, D. Moosmayer, A. Hilppmann, M.J. Ryan, K. Zimmermann, L.L. Cai, M. Niehues, V. Badock, A. Kramm, S. Chen, R.C. Hillig, P. A. Clemons, S. Gradl, C. Montagnon, K.E. Lazarski, S. Christian, B. Bajrami, R. Neuhaus, A.L. Eheim, V.S. Viswanathan, S.L. Schreiber, Selective covalent targeting of GPX4 using masked nitrile-oxide electrophiles, *Nat. Chem. Biol.* 16 (2020) 497–506.
- [54] R.D. Leone, L. Zhao, J.M. Englert, I.M. Sun, M.H. Oh, I.H. Sun, M.L. Arwood, I. A. Bettencourt, C.H. Patel, J. Wen, A. Tam, R.L. Blosser, E. Prchalova, J. Alt, R. Rais, B.S. Slusher, J.D. Powell, Glutamine blockade induces divergent metabolic programs to overcome tumor immune evasion, *Science* 366 (2019) 1013–1021.
- [55] M.H. Oh, I.H. Sun, L. Zhao, R.D. Leone, I.M. Sun, W. Xu, S.L. Collins, A.J. Tam, R. L. Blosser, C.H. Patel, J.M. Englert, M.L. Arwood, J. Wen, Y. Chan-Li, L. Tenora, P. Majer, R. Rais, B.S. Slusher, M.R. Horton, J.D. Powell, Targeting glutamine metabolism enhances tumor-specific immunity by modulating suppressive myeloid cells, *J. Clin. Invest.* 130 (2020) 3865–3884.
- [56] Y. Yokoyama, T.M. Estok, R. Wild, Sirpiglenastat (DRP-104) induces antitumor efficacy through direct, broad antagonism of glutamine metabolism and Stimulation of the Innate and adaptive immune systems, *Mol Cancer Ther* 21 (2022) 1561–1572.
- [57] L. Yang, S. Venneti, D. Negrath, Glutaminolysis: a hallmark of cancer metabolism, *Annu. Rev. Biomed. Eng.* 19 (2017) 163–194.